

Novel spherical boron clusters and structural transition from 2D quasi-planar structures to 3D double-rings

Saikat Mukhopadhyay¹, Haying He¹, Ravindra Pandey¹, Yoke Khin Yap¹ and Ihsan Boustani²

¹ Michigan Technological University, Department of Physics, Houghton, Michigan, 49931 USA

² Bergische Universität Wuppertal, FB C - Mathematik und Naturwissenschaften, Gaußstraße 20, D-42097 Wuppertal, Germany

E-mail: boustani@uni-wuppertal.de

Abstract. Based on *ab initio* quantum-chemical and density functional methods we determined the geometry, electronic and structural properties of three cluster-families: boron spheres, double-rings and quasi-planars up to a cluster size of 122 atoms. The most stable structure is the B₁₀₀ sphere showing similar shape but more stability than the B₈₀ cage recently proposed by Yakobson *et al* [PRL 98, 166804 (2007)]. In addition we compared the stability of the three cluster families to each other, and reported the structural transition from 2D quasi-planar clusters to 3D double-rings. This transition occurs between the B₁₆ and B₁₉ clusters.

1. Introduction

The ultimate goal of this research field is to develop, simulate and predict new arrays of nanoclusters and nanotubes with desired, pre-selected and specific uniform properties. The incorporation of nanoclusters, nanotubes and nanocrystals into nanostructured materials can be expressed in form of miniaturization of these new materials and could lead to nanoscaled electronic devices. For instance, possible application fields are in oil-industry, medicine and materials science. During the last decade many researchers focused on a systematic search for new materials mainly consisting of pure or mixed boron, carbon, nitrogen, boron-hydrogen and metal-boron types of systems [1, 2].

Though some variety of possible structures in nanostructured materials like quasi-crystals [3], nanowires [4], nanoribbons [5], was identified, many forms however remain to be discovered. In order to achieve this, there are several theoretical methods based on a variety of concepts, ranging from the most accurate *ab initio* first-principle methods suited for small or medium sized systems to semi-empirical methods for very large systems. Those methods are reliable tools to detect, to analyze and optimize most of materials, and in many cases they already turn out to be some sort of inexpensive, fast and reliable alternative to standard experimental methods in materials science. These methods provide an opportunity for 'materials engineering', a systematic understanding and development of new nanoscale materials with desired properties. Ultimately, an understanding of "self-assembling" of boron-based materials could lead to manufacturing of useful structures [6].

The physics and chemistry of boron resembles in its ability to configure and form molecular networks. Unlike carbon, bulk boron cannot be found in nature and all known boron allotropes were obtained in the laboratory. All of them are based on different arrangements of B_{12} icosahedra. It is very natural to believe that - like carbon - boron also can form molecular allotropes (fullerenes and nanotubes). Experimental and theoretical research on the chemistry of boron nanomaterials is developing rapidly. The existence of quasi-planar [7] and tubular [8] boron clusters was predicted theoretically and confirmed more recently experimentally [9, 10]. In addition, double-walled boron nanotubes were predicted to be highly stable [11]. These authors found that the interaction between the walls in form of σ -bonds increases the stability of the system in opposite to the carbon nanotubes where the walls are connected by Van-der-Waals forces only, in which no chemical bonds are formed among the neighboring walls.

Lipscomb and co-workers proposed boron spheres as large closo boron hydrides in an analogon to carbon fullerenes using the Descartes-Euler formula $P + F = E + 2$ (P for vertices, F for faces, and E for edges) [12]. They also predicted “conjuncto closo boranes” and their relationships to the dual structures [13]. Based on quantum chemical methods they extended their studies and proposed multicage boron fullerenes B_nH_n [14, 15]. A new concept of conjugate polyhedra was introduced by Tang *et al* [16]. Considering the above Descartes-Euler formula and by a given polyhedron of carbon (boron) one can obtain the corresponding conjugate polyhedron of carbon (boron) by interchange of P and F , with E being kept constantly. These conjugate polyhedra share the same symmetry. For example, for the icosahedral symmetry group I_h , B_n : $n = 30 k^2 + 2$ is the conjugated polyhedron to carbon C_n : $n = 60 k^2$. In other words, one can determine for carbon fullerenes C_{60} , C_{240} , the corresponding boron spheres to be B_{32} , B_{122} , for $k = 1$ and 2 , respectively.

Small pure boron spheres were predicted by Boustani [17]. Besides the icosahedron B_{12} he constructed small boron B_{22} , B_{32} and B_{42} cages, based on the “Aufbau Principle” [7] as a combination of pentagonal and hexagonal pyramids. In addition, spherical boron hydrides were the subject of a further study by Boustani *et al* [18]. They attached hydrogen atoms to the boron spheres and concluded that the idea of Lipscomb and Massa for geometrical mapping between fullerenes and boron is consistent with the ab initio proved proposals. Besides their equality in the number of carbon faces and boron vertices and vice versa we may add another equality to generate new boron spheres in the way that the number of vertices and faces of carbon can be replaced by boron vertices.

A new strategy to define reliable geometries for spherical boron cages without resorting to complicated and heavy ab initio calculations was presented by Amovilli and March [19]. Their method reflects the “Aufbau Principle” proposed for boron clusters but it is not restricted to a series of magic numbers. It is always possible, in fact, to recover a sphere with distorted pentagons and hexagons not necessarily displaced in an ordered manner. This situation coincides with the projection - over the surface of the sphere - of the faces of a polyhedron generated by a system of equal charges, with the motion constrained over the sphere surface itself, in their more stable configuration. Such geometries can be easily generated for a given number n of boron atoms by a simple Monte Carlo sampling in a few minutes. The radius R_e of the sphere, however, is finally found by imposing a constant numeral surface density $n/4\pi R_e^2$ [19].

Recently boron fullerenes were presented by Yakobson *et al* [20]. Based on ab initio first-principle methods they generated spherical boron cages as a combination of several staggered double-rings crossing together in a rhombus. The energies of the spheres were compared to the corresponding reference energies of the double-rings. They found that the B_{80} cage, with a binding energy per atom of 5.76 eV, was the most stable sphere symmetrically similar to the C_{60} structure. The only difference between B_{80} and B_{60} is the presence of an additional atom at the center of each hexagon. These facets of the B_{80} follow the “Aufbau Principle” although the hexagonal pyramidal units are rather planar here.

Larger fullerenes with a cluster size of up to B_{300} were proposed by Szwacki [21], using ab initio DFT methods. These cages have similar structures consisting of six interwoven boron double-rings. He predicted that the most stable fullerene is made up of 180 atoms and has almost a perfect spherical shape and is more stable than the B_{80} fullerene by 0.01 eV. He also showed that each fullerene of B_{80} , B_{180} , and B_{300} is accompanied by its precursor sheet. The sheets have atomic motifs with a C_{3v} symmetry, similar to the quasi-planar B_7 , B_{12} and B_{18} clusters. The precursor sheets of B_{80} , B_{180} , and B_{300} exhibit holes characterized respectively by 6, 9 and 12 surrounding atoms. The existence of holes in very stable α -sheets was already proposed by Tang and Ismail-Beigi [22].

Furthermore, the spherical B_{84} cluster, known as a subunit of β -boron, as well as the B_{156} cluster were experimentally observed by Oku [23]. Both clusters were directly detected by high-resolution electron microscopy and crystallographic image processing, embedded in $B_{105}Al_{2.6}Cu_{1.8}$ and $B_{56}Y$ crystals. The detection technique, developed by Oku [23], seems to be useful for evaluation of the arrangement of light elements like boron clusters. However, a recent ab initio DFT study presented by Prasad and Jemmis [24] claims that stuffing of fullerene-like boron clusters leads to improving their stability. The authors showed that boron clusters such as B_{98} , B_{99} , B_{100} , B_{101} , B_{102} based on icosahedral B_{12} stuffed fullerenes are more stable than the hollow clusters. The most stable fullerene-like cluster was the B_{101} cage, which is around 0.081 eV more stable than the Yakobson's B_{80} fullerene. The basic idea arises from the spherical B_{84} cluster which was extracted from β -rhombohedral boron. The B_{84} is a stellation of B_{12} icosahedron and of 12 B_6 pentagonal "umbrellas". The authors said that the B_{84} is deficient by 50 electrons according to the Wades $n+1$ and $n+2$ skeletal electron rules [25]. The 50 electron deficient B_{84} cluster can be stabilized by adding 16.66 atoms to be made electron sufficient. Therefore, the clusters surrounding $B_{100.66}$ should be the right candidates.

Further study on a bundle of B_{80} fullerenes condensed to a face-centered-cubic solid was carried out by Yan, Zheng and Su [26]. They showed that when forming a crystal, the icosahedral structure of the B_{80} cages is distorted leading to lowering the symmetry from I_h to T_h . They also found that there are chemical bonds between the nearest neighboring five B_{80} clusters in (001) plane. The interaction between these cages improves the stability so that the cohesive energy of the fcc B_{80} solid is about 0.23 eV/atom with respect to the isolated B_{80} fullerenes. They also proposed a different electron counting rule which could might explain the stability of the B_{80} fullerene. They considered that each triangle would consume two electrons in a three-center two-electrons bond ($3c2e$) while no electrons are considered by the 12 pentagonal holes. For 120 triangles (6 triangles for each of 20 hexagons) there are 240 electrons required for bonds. This number is equal to the number of the valence electrons of the B_{80} . In other words, this rule says that the number of the total electrons demanded for bonding should be equal to the total number of the valence electrons. Another interesting result of their calculations is that the electronic structure reveals the fcc B_{80} solid to be metallic.

In this paper we will report on the structures of three cluster families: i) of nearly round boron cages built from pentagons and hexagons or from pentagonal and hexagonal pyramids, ii) of double-rings (DR), and iii) of quasi-planar (QP) clusters, up to a cluster size of 122, and of the structural transition from 2D quasi-planar clusters to 3D double-rings in comparison to an infinite boron strip. The results will be finally discussed and the main conclusions will be given.

2. Theoretical Details

The calculations for the current work were performed using ab initio first-principle methods for solving the many-electron problems in atoms, clusters, and solids, in the framework of the Hartree-Fock (HF) self-consistent-field (SCF) and the density functional theory [27, 28]. These important concepts are the kernels of a variety of program packages that we use for our

simulations, depending on the size of the system to be examined. Due to the fact that the size of the investigated systems is relatively large, it was advisable to use the standard minimal STO-3G basis set to calculate large systems containing over 100 atoms and to consider symmetry constraints in the form of a point group symmetry. The optimization process was carried out at the nonlocal corrections to exchange correlation B3LYP [29, 30], using the program packages GAMESS_UK [31] and Gaussian 03 [32].

In the present contribution, the geometrical and electronic structures of the boron clusters B_n for $n = 12 - 122$ were investigated. Only the final geometries of the lowest energy selected cluster are presented. The optimization procedure, based on the analytical gradient method, was carried out for the ground state energies using the restricted Hartree-Fock theory, followed by B3LYP throughout. In order to compare the stability of all clusters we calculated the binding energy per atom which is defined as $(E_b = E_1 - E_n/n)$, where n is the cluster-size, E_1 is the energy of atomic boron, and E_n is the cluster energy. Since the geometrical structures of the clusters influence their electronic properties we compared their highest occupied molecular orbital (HOMO) and the lowest unoccupied molecular orbital (LUMO) in relationship with the cluster size.

3. Results and discussion

3.1. Boron Spheres

Inspired by Yakobson *et al* [20], our investigations on larger boron spheres were carried out using the ab initio methods mentioned above. We considered spherical boron clusters B_n for $n = 12, 20, 32, 42, 60, 72, 80, 92, 100, 110, \text{ and } 122$, most of them with icosahedral symmetry [figure 1]. The cage B_{12} is the well known icosahedron of the α -rhombohedral crystalline boron.

Table 1. The considered spherical boron clusters [figure 1] and the corresponding binding energy per atom E_b , obtained at the B3LYP-STO3G level of theory

Cluster	Symmetry	E_b (eV)	Number of		
			Triangles	Pentagons	Hexagons
B_{12}	I_h	5.68	20	12	-
B_{20}	I_h	6.07	-	12	-
B_{32}	I_h	6.12	60	12	12
B_{42}	D_{5d}	6.27	70	12	20
B_{60}	I_h	6.42	-	12	20
B_{72}	I_h	6.63	60	12	20
B_{80}^h	I_h	6.65	-	12	30
B_{80}^f	I_h	6.72	120	12	20
B_{92}	I_h	6.70	180	12	20
B_{100}	D_{5d}	6.81	120	12	30
B_{110}	I_h	6.53	180	12	30
B_{122}	I_h	6.19	240	12	20
${}^a B_{12}$	C_{3v}	6.29			
${}^b \text{Strip}$	C_1	6.78			
${}^c B_{81}$	D_{2h}	6.39			
${}^d \alpha\text{-Boron}$	I_h	7.66			

^a The quasi-planar structure [figure 2], ^b The infinite strip [figure 5], ^c Precursor Sheet of B_{100} [figure 6], ^d Crystalline rhombohedral boron.

The structure of $B_{12} - I_h$ has 12 vertices and 20 faces. It has a binding energy per atom E_b of 5.68 eV, calculated at the STO3G-B3LYP level of theory. However, since the five-fold degenerate HOMOs of B_{12} are not fully occupied the Jahn-Teller-effect follows and distorts the icosahedral

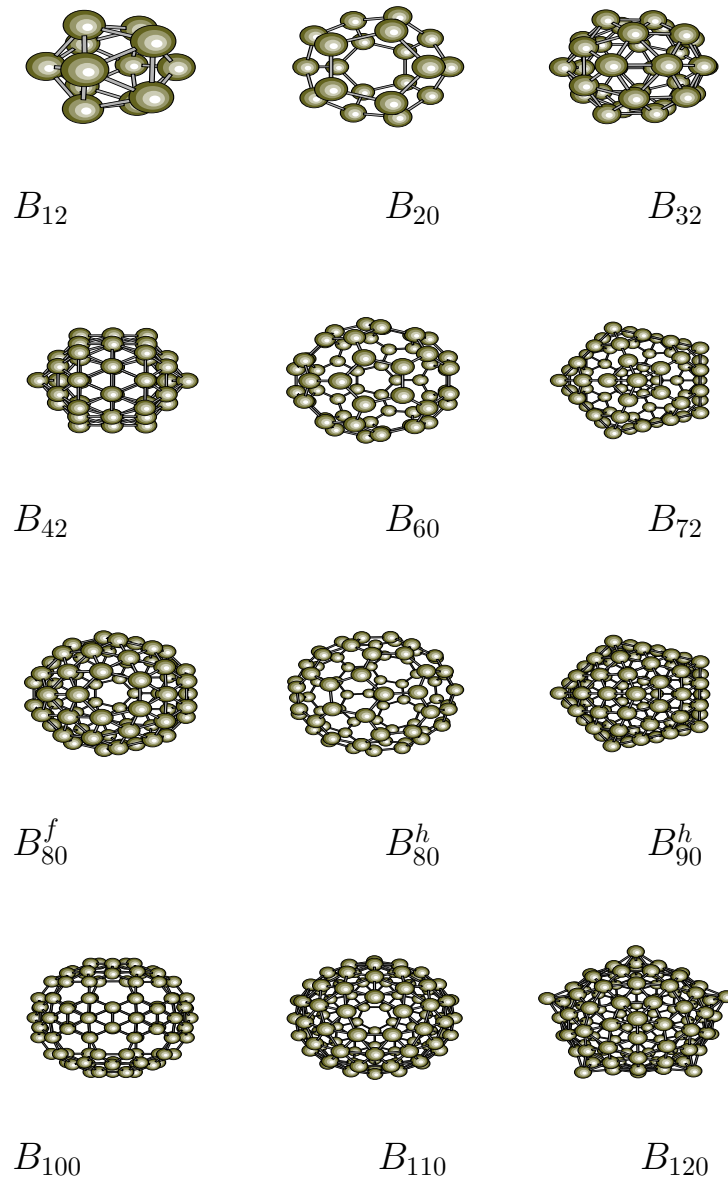


Figure 1. Spherical structures of the B3LYP-optimized boron clusters B_n , obtained with the STO3G basis set. The symmetry point group of the clusters is I_h except of B_{42} and B_{100} clusters which have D_{5d} symmetry.

symmetry to a lower one so that the icosahedron flats out into a quasi-planar structure of C_{3v} symmetry [figure 2] approaching a high stability of 6.29 eV [table 1]. The dodekahedron B_{20} , with a E_b of about 6.07 eV, has 20 vertices but 12 faces, in opposite to the icosahedron. Both structures, icosahedron and dodekahedron have 30 edges regarding the Descartes-Euler formula mentioned above.

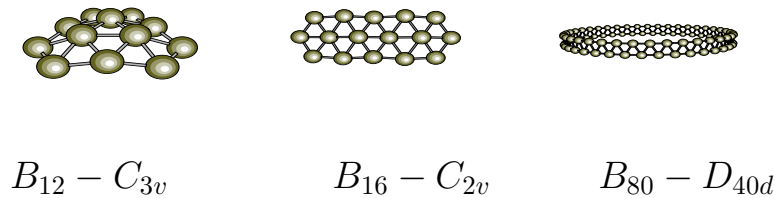


Figure 2. Examples of quasi-planar and double-rings structures of obtained at the B3LYP-STO3G level of theory.

Fusing both the icosahedral and dodecahedral cages we receive the $B_{32} - I_h$ which has 30 faces and 60 edges. It can be seen as dovetailed 12 pentagons and 12 hexagons. The E_b of the B_{32} cage is around 6.12 eV. The $B_{42} - D_{5d}$ sphere can be generated by adding an atomic ring of 10 boron atoms perpendicular to an arbitrary axis going through two polar atoms of the $B_{32} - I_h$ cage. The B_{42} structure has 70 faces and 110 edges. The binding energy per atom of the B_{42} increases to 6.27 eV. The $B_{60} - I_h$ cage can be achieved by replacing each icosahedral atom in $B_{12} - I_h$ by a pentagonal B_5 cluster keeping the icosahedral symmetry. Its geometry is simply that one of the C_{60} fullerene. The related E_b is about 6.43 eV. The structure $B_{72} - I_h$ arises from $B_{60} - I_h$ by setting one boron atom in each center of the 12 pentagons. The binding energy per atom of the B_{72} cage is around 6.63 eV.

There are two structures of B_{80} both with I_h symmetry. The first but less stable one called hexagonal B_{80} (B_{80}^h) can be generated by rotating the pentagons in B_{60} , so that the edges of neighboring pentagons are parallel, then adding a dodecahedron B_{20} having the same radius. This $B_{80}^h - I_h$ cage has the same form as the C_{80} fullerene. The B_{80}^h structure has 42 faces (12 pentagons and 30 hexagons). The number of hexagons n can be calculated after ($n = a/2 - 10$), where a is the number of boron atoms of the sphere. This B_{80}^h structure is the starting geometry for the most stable cage B_{100} . The other and more stable structure B_{80} fullerene (B_{80}^f) was proposed by Yakobson et. al. [20]. It can be generated by adding one boron atom to each center of the 20 hexagons of the B_{60} fullerene. The binding energy per atom of B_{80}^f is nearly 6.72 eV. The average radius (AR) of the cage is about 4.15 Å.

The structure $B_{92} - I_h$ is arising from $B_{60} - I_h$ by setting one boron atom to each center of the 12 pentagons and 20 hexagons of the B_{60} fullerene. The corresponding E_b is about 6.70 eV with an AR of 4.7 Å. The cages $B_{100} - D_{5d}$, and $B_{110} - I_h$ can be obtained by setting 20 and 30 boron atoms into the centers of the hexagons of the B_{80}^h cage, respectively. The calculated binding energy per atom for B_{100} is 6.81 eV and for B_{110} is about 6.53 eV and their AR is about 5 Å. Finally, the cage B_{122} can be generated by setting boron atoms to each center of the 12 pentagons of the B_{110} cage. B_{122} seems to be less stable than the previous one and has a E_b of about 6.28 eV and an AR of 5.19 Å. For comparison, the cohesive energy of the periodic rhombohedral α -boron, calculated at B3LYP-STO3G, is about 7.66 eV/atom.

In order to assess the idea of Tang and Ismail-Beigi [22] which says that the hexagonal holes (defects) enhance more stability in boron sheets and nanotubes, we determined the cages between B_{80} and B_{110} by gradually adding two atoms to two centers of these 30 hexagons of B_{80}^h . We found out that filling only 20 hexagons of a maximum of 30 leads to the highest stability of all structures [figure 4]. In other words, the spherical B_{100} cage seems to be the most stable cluster between all 2D and 3D clusters and the idea of holes is working well. The B_{100} sphere is consisting of a ring of 10 centered hexagons bicapped by five connected centered hexagons.

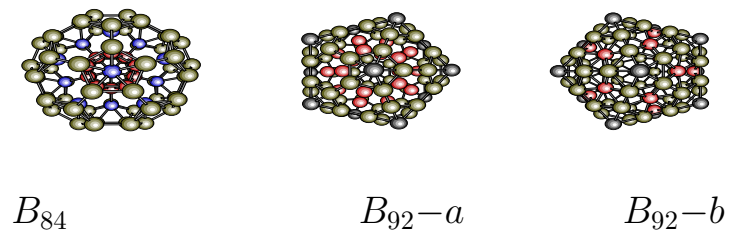


Figure 3. The B_{84} cage is composed of three shells: B_{12} (red), B_{12} (blue) and B_{60} (green). The B_{92} cages give an example for stretching the inner shell depicted by the nonbonding dodecahedron (red balls) in B_{92-a} outwards to the external shell B_{92-b} forming new chemical bonds.

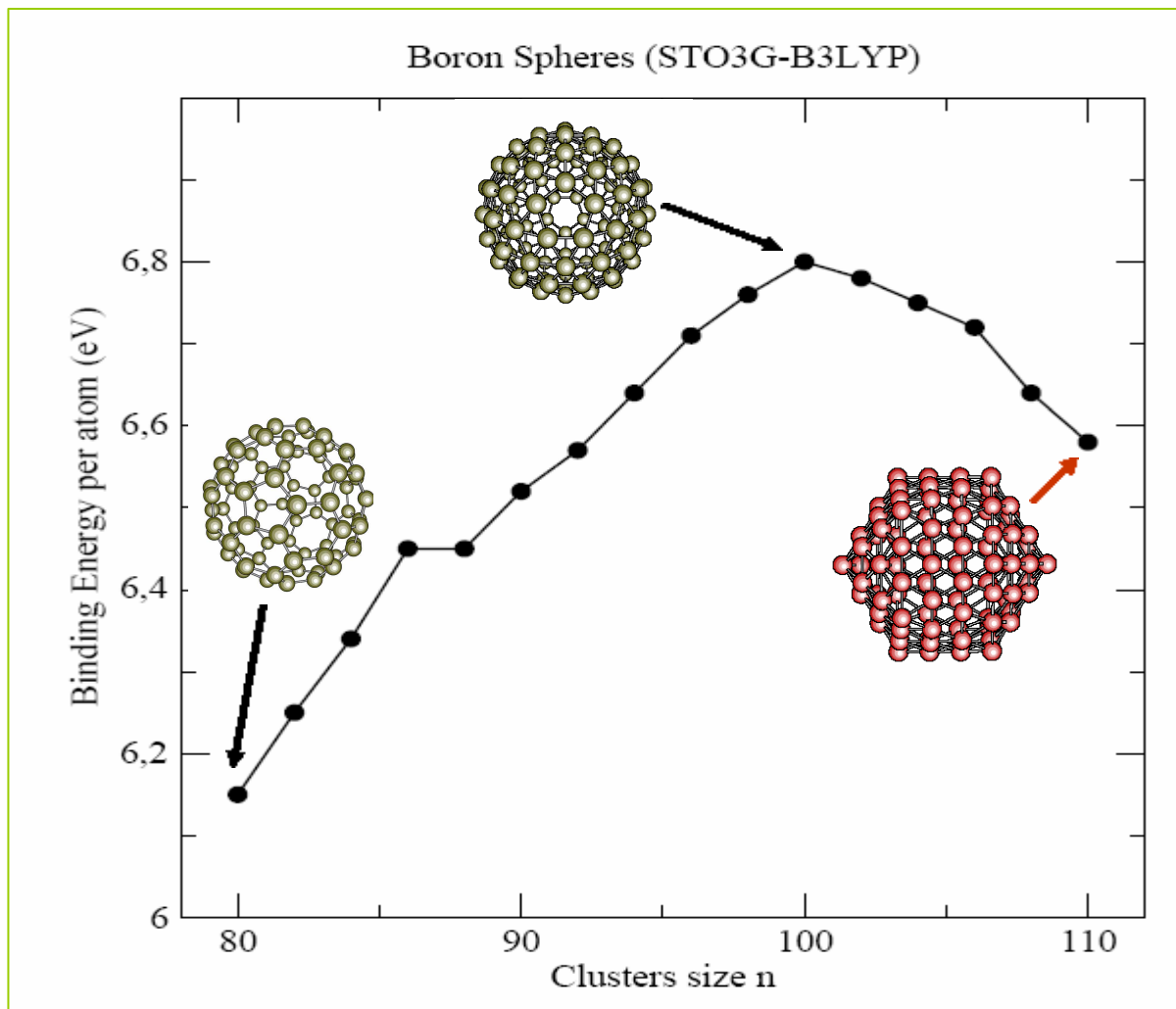


Figure 4. Binding energy per atom as a function of the cluster size n of B_n for $n = 80$ to 120 , via adding two by two boron atoms in each of the 30 hexagonal centers of the spherical B_{80}^h cluster.

This B_{100} sphere is accompanied by a segment of its precursor sheet [figure 6.]. This sheet (B_{81} with a D_{2h} symmetry) is by 0.42 eV less stable than the B_{100} sphere.

Furthermore, we studied few spherical clusters composed of different shells [see figure 3]. The first one, a B_{84} sphere, is consisting of two shells: $B_{12}@(B_6)_{12}$. The inner shell B_{12} is an icosahedron connected to 12 pentagonal pyramids in a form of open umbrellas B_6 , considered as the outer shell. The calculated binding energy per atom is about 6.43 eV and lies below the corresponding E_b of B_{80}^f which is 6.72 eV. Further examples for stuffing are the B_{92} isomers, illustrated in [figure 3]. The sphere $B_{92} - a$ is consisting of an inner shell B_{20} which is not connected to the outer shell of B_{72} . The inner shell stretches outward and leans forward to build up new chemical bonds with the outer shell, as can be seen by the $B_{92} - b$ cluster.

It was determined experimentally that the QP B_{12} has a relatively large HOMO-LUMO gap of 2.0 eV [9]. Theoretically, the HOMO-LUMO gap of the QP B_{12} according to our calculations is about 2.47 eV which is the largest gap of all clusters. The HOMOs and the LUMOs of the spherical cluster B_{80} are both fivefold degenerate exhibiting a gap of 2.27 eV, being the next largest value. It is comparable to the value of 1.94 eV calculated by Gopakumar [33] for the buckyball B_{80}^f . The estimated gap of the B_{80}^f cage, obtained by Yakobson [20], amounts to 1.01 eV, nearly to less than the half of the previous values. In contrast, the gap of the B_{100} sphere is of a relatively small value 0.14 eV. That can be connected with the symmetry of the cluster. When the HOMOs are degenerate and fully occupied the cluster exhibits a large HOMO-LUMO gap, as in the case of the B_{80}^f cage. But when these orbitals are partially occupied, the degeneracy finishes and the gap is small, as in the case of the B_{100} sphere. In general the HOMO-LUMO gaps of all clusters are alternating as a function of the cluster size in a decreasing manner approaching small values for larger cluster sizes converging to be metallic as in the case of the infinite boron strip.

3.2. Boron Double-Rings

Regarding our previous studies on segments of single-walled boron nanotubes with different diameters and sizes, we found that staggered double-rings of the following boron clusters B_{24} [34], B_{32} [35], B_{36} [36], and B_{96} [37] have the highest stability compared to all other multi-ring structures. In order to study the stability of the boron double-rings family in relationship to the cluster-size, we carried out new ab initio calculations starting from the smallest DR B_{12} up to the largest DR of B_{122} . An example of these structures is given in [figure 2]. We optimized these structures at the B3LYP and STO3G level of theory. The stability of these structures, expressed as the binding energy per atom, increases with increasing cluster-size, which is shown in [figure. 5]. We also calculated the energy of an infinite strip of double-rings as a reference for all structures. The binding energy per atom of this infinite structure is 6.78 eV.

In comparison of the double-rings and spherical structures of B_{80} and B_{100} clusters we found that the binding energy per atom obtained for the B_{80} DR, calculated at the HF-SCF and B3LYP level of theory, are 5.39 eV and 6.75 eV, respectively. They are higher than the corresponding ones 5.22 eV and 6.74 eV, determined for the spherical B_{80}^f . This means that the DR of B_{80} is more stable than the spherical one at both levels of theory. Concerning the B_{100} structure, the E_b of B_{100} DR obtained at the HF-SCF level is about 5.39 eV, while the corresponding E_b of the spherical B_{100} cluster is 5.27 eV. At the more reliable B3LYP level of theory we have a reverse picture. The E_b of B_{100} DR is about 6.77 eV while the B_{100} sphere is 6.81 eV. In other words, the B_{100} DR is more stable at the HF-SCF level than the B_{100} sphere, while the sphere is more stable at the B3LYP level of theory due to its high correlation energy.

3.3. Quasi-planar Clusters and Structural Transition

It was established that different boron cluster topologies in form of quasi-planars, sheets or nanotubes possess highly stable structures. It was also found that the most stable boron clusters are small and have quasi-planar structures. But what happens with growing the cluster size? Therefore the simple question rises: Up to which size do the 2D quasi-planar structures remain as the most stable ones? This item was the subject of further studies exploring the transition from 2D to three-dimensional (3D) structures. Kiran *et al* [38] proposed B₂₀ as the embryo of single-walled boron nanotubes for a planar-to-tubular structural transition in boron clusters. They investigated experimental and computational simulation methods revealing that boron clusters, which favour planar 2D structures up to 18 atoms, prefer 3D structures beginning at 20 atoms.

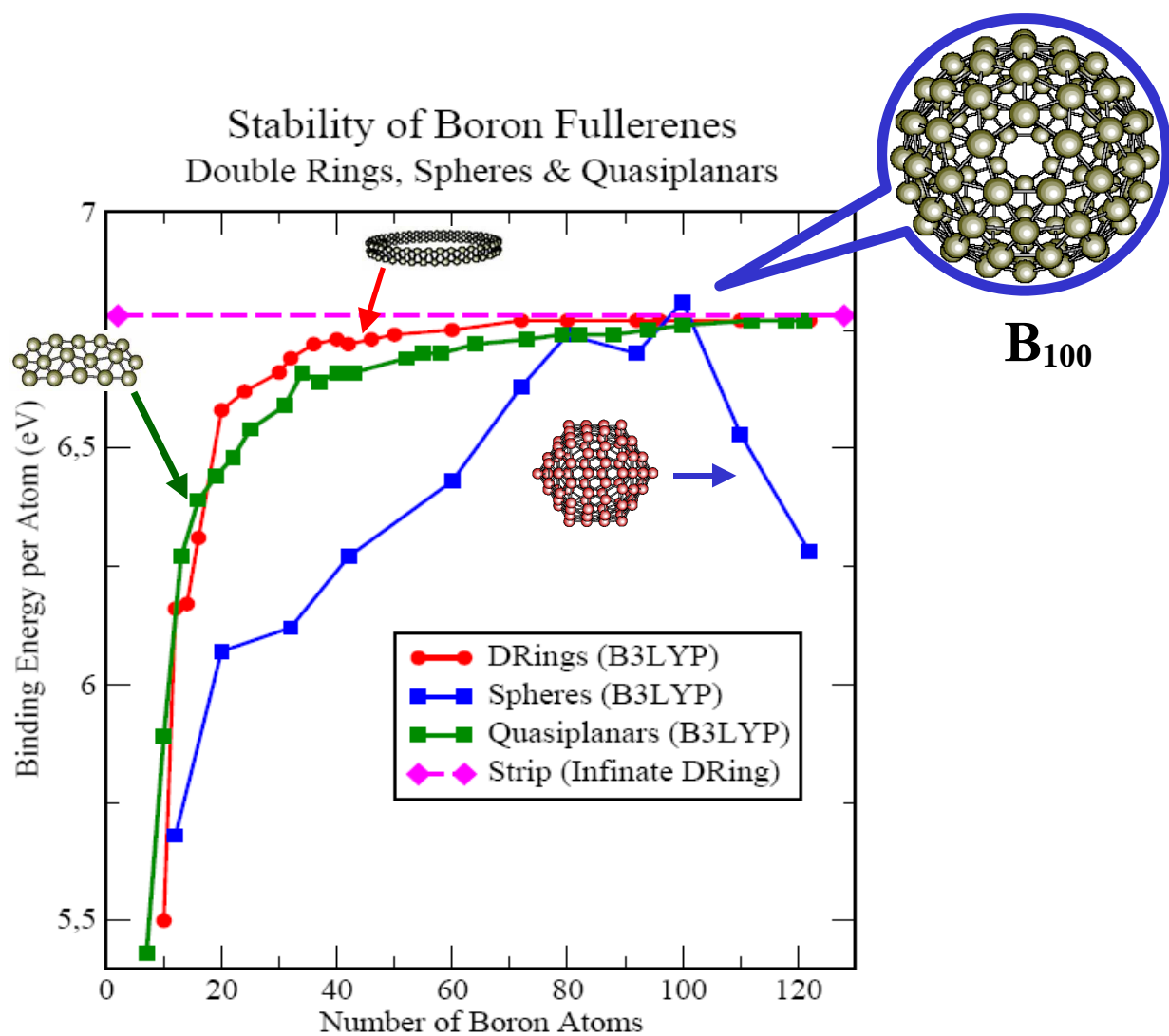


Figure 5. Binding energy per atom as a function of the cluster size for spherical, quasi-planar, and double-ring boron clusters showing other perspective of the spherical B₁₀₀ cluster namely along the 5-fold symmetry axis.

Marques and Botti [39] examined the structural transition question from the optical point

of view. They applied the time-dependent density functional theory using the real-time and space to solve the time-dependent Kohn-Sham equations. They also showed that the optical spectroscopy can be applied to distinguish without ambiguity between the different low-energy members of the B_{20} family. The most stable neutral B_{20} isomer is the tubular cluster which can be unequivocally identified due to the presence of a very sharp resonance at about 4.8 eV.

An *et al* [40] studied the relative stability among four low-lying isomers of neutral and anionic B_{20} clusters. They carried out highly accurate MP4(SDQ) and CCSD(T) calculations yielding the same energy ordering for the neutral B_{20} isomers. Both calculations show that the double-ring is the lowest-energy structure, has a large negative nucleus-independent chemical shift and therefore is strongly aromatic. Oger *et al* [41] asserted that boron cluster cations were found to undergo a transition between quasi-planar and cylindrical molecular structures at B_{16}^+ . The experimentally determined collision cross sections are consistent with those calculated for the global minimum structures as obtained from the theory. For the cations B_{17}^+ and larger, the cylindrical geometries dominate the low-energy structures and for neutral clusters, the transition from 2D to double-ring structures occurs for B_{20} .

As mentioned above, several authors [38] to [41] showed theoretically and experimentally that a structural transition from 2D into 3D structures occurs between B_{16} and B_{20} . Therefore, we investigated different configurations of quasi-planar clusters starting from B_{12} in gradual steps of three atoms up to B_{122} quasi-planar clusters using the same theoretical methods mentioned in section II. An example of quasi-planar clusters is shown in [figure 2]. The calculations of the quasi-planar clusters expressed in form of binding energy per atom are shown in [figure 5]. One can recognize that the binding energies of the 2D quasi-planar clusters are crossing those of the 3D structures of double-rings confirming that the structural transition from 2D into 3D occurs between the B_{16} and B_{19} clusters.

4. Discussion and Conclusions

We developed novel structures in the form of spheres, double-rings and quasi-planar structures. These nanostructures were optimized at the B3LYP level of theory using the STO3G basis set. Generally, the optimized boron spheres range from the smallest B_{12} icosahedron to B_{20} , B_{32} , B_{42} , B_{60} , B_{72} , B_{80} , B_{92} , B_{100} , B_{110} and up to B_{122} . The average radius of the spheres are between 4.15 and 5.19 Å and the interatomic distances are about 1.67 to 1.94 Å. We also optimized double-rings as segments of nanotubes from a DR of B_{12} ($2xB_6$) up to a DR of B_{122} ($2xB_{61}$). In addition we studied two-dimensional structures in the form of quasi-planar clusters from 12 up to 122 cluster size. The smallest QP cluster is the $B_{12} - C_{3v}$, the conjugate of the icosahedron. The next QP cluster is the $B_{16} - C_{2v}$ strip which is composed of three parallel staggered chains [figure 2]. Further QP clusters are generated in gradual steps by adding three atoms to each cluster up to the largest one B_{122} .

We conclude that the most stable clusters is the B_{100} sphere whose binding energy per atoms goes behind that of the infinite strip of the DR clusters. The structure of B_{100} contains triangle and hexagonal motives. These motives contribute essentially to the cluster stability as recently found in boron sheets [43]. Our B_{100} sphere is about 0.09 eV more stable than the B_{80}^f proposed by Yakobson. Similar value of around 0.081 eV obtained by Jemmis for the stuffed B_{101} structure in relationship to Yakobson B_{80}^f cage. “Stuffing improves the stability” of boron clusters proposed by Jemmis could not be confirmed by our the B_{84} and B_{92} clusters. However our B_{100} is one of the favourites determined by the counting rules and fulfills the stability requirement to stabilize B_{84} by adding exact 16 atoms. Furthermore, our B_{100} sphere does not fulfill the counting rules proposed by Su *et al* [26]. The B_{100} sphere has 120 triangles 3c2c bonds consuming 240 electrons and 20 two-center two-electron 2c2e bonds counting two 2c2e for each of the 10 hexagonal holes, consuming 40 electrons. The sum of the required electrons 280 is not equal to the valence

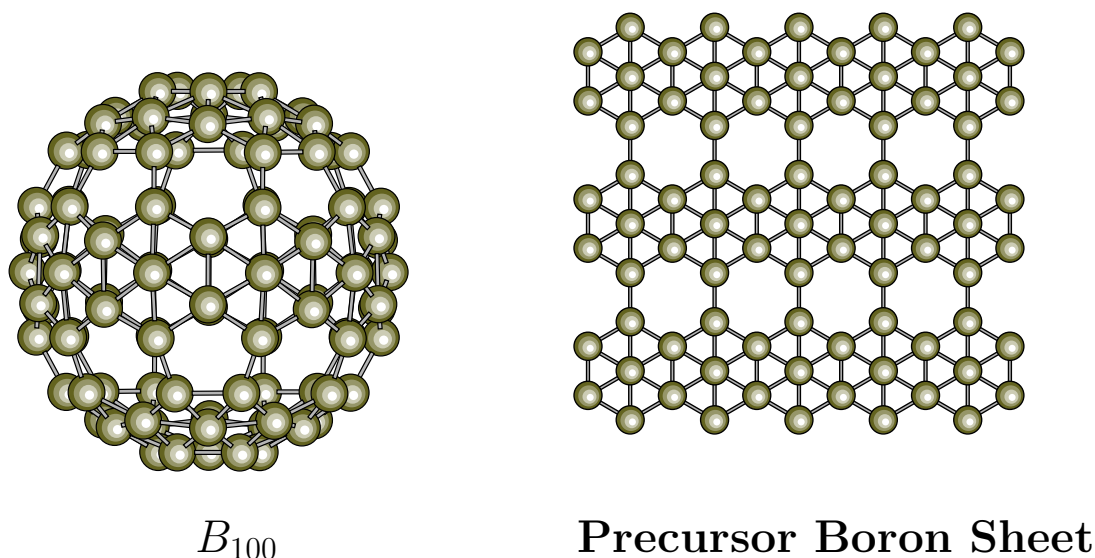


Figure 6. The spherical B_{100} cluster and the related precursor boron sheet. The structure of B_{100} is composed of ten dovetailed equatorial centered hexagons consisting 50 atoms and two polar cups each is consisting of five dovetailed centered hexagons with 25 atoms.

electrons of B_{100} .

The structural transition from 2D quasi-planar clusters into 3D double-rings occurs beyond the B_{16} cluster and is in excellent agreement with the experimental results obtained by Oger *et al* [41], determined by photoelectron spectroscopy. Furthermore, the quasi-planar structure of B_{16} is identical to that one found experimentally by Sergeeva *et al* [42]. Finally, the most stable sphere B_{100} has a small HOMO-LUMO gap and less stable precursor sheet in opposite to the less stable B_{80} fullerene with a relatively larger HOMO-LUMO gap and very stable precursor α -sheet. In other words, the most stable structure of the spheres does not necessarily have a very stable precursor sheet or to exhibit a large HOMO-LUMO gap. The both precursors of B_{80}^f and B_{100} spheres are only two of many pattern which could be generated by different combinations of hexagonal holes of the precursor sheets. Since there exists at least more than one precursor for the stable B_{100} sphere, we believe that the energy of this cage corresponds to one of the local minima on the potential energy hypersurface of these clusters. Therefore, further investigations are required to search for the global minimum, electronic, and thermodynamic properties.

References

- [1] Terrones M 2004 *Int. Mater. Rev.* **49** 325
- [2] Ivanovskii A L 2002 *Russ. Chem. Rev.* **71** 175
- [3] Boustani I, Quandt A, and Kramer P 1996 *Europhys. Lett.* **36** 583
- [4] Zhang Y, Ago H, Yumura M, Ohshima S, Uchida K, Komatsu T and Iijima S 2004 *Chem. Phys. Lett.* **385**

- [5] Ding Y, Yang X and Ni J 2008 *Appl. Phys. Lett.* **93** 043107
- [6] Quandt A and Boustani I, and the references therein in 2005 *Minireviews, ChemPhysChem* **6** 1
- [7] Boustani I 1997 *Phys. Rev. B* **55** 16426
- [8] Boustani I, Quandt A, Hernandez E and A. Rubio 1999 *J. Chem. Phys.* **110** 3176
- [9] Zhai H J, Kiran B, Li J and Wang L-S 2003 *Nature Mat.* **2** 827
- [10] Ciuparu D, Klie R F, Zhu Y and Pfefferle L 2004 *J. Phys. Chem. B* **108** 3967
- [11] Sebetci A, Mete E and Boustani I 2008 *J. Phys. Chem. Solid* **69** 2004
- [12] Lipscomb W N and Massa L 1992 *Inorg. Chem.* **31** 2299
- [13] Lipscomb W N and Massa L 1994 *Inorg. Chem.* **33** 5155
- [14] Derecskei-Kovacs A, Dunlap B I, Lipscomb W N, Lowrey A, Marynick D S and Massa L 1994 *Inorg. Chem.* **33** 5617
- [15] Gindulyte A, Krishnamachari N, Lipscomb W N and Massa L 1998 *Inorg. Chem.* **37** 6546
- [16] Tang A-C, Li Q-S, Liu C-W and Li J 1993 *Chem. Phys. Lett.* **201** 465
- [17] Boustani I 1997 *J. Solid State Chem.* **133** 182
- [18] Boustani I, Rubio A and Alonso J A 2000 *Contemporary Boron Chemistry* (eds) M G Davidson, A K Hughes, T B Marder and K Wade (the Royal Society of Chemistry, Cambridge) p 493
- [19] Amovilli C and March N H 2001 *Chem. Phys. Lett.* **347** 459
- [20] Szwacki N G, Sadrzadeh A and Yakobson B 2007 *Phys. Rev. Lett.* **98** 166804
- [21] Szwacki N G 2008 *Nanoscale Res. Lett.* **3** 49
- [22] Tang H and Ismail-Beigi S 2007 *Phys. Rev. Lett.* **99** 115501
- [23] Oku T 2003 *Solid State Commun.* **127** 689
- [24] Prasad D L V K and Jemmis E D 2008 *Phys. Rev. Lett.* **100** 165504
- [25] Wade K 1971 *J. Chem. Soc. D* **15** 792
- [26] Yan Q-B, Zheng Q-R and Su G 2008 *Phys. Rev. B* **77** 224106
- [27] Hohenberg P and Kohn W 1964 *Phys. Rev. B* **136** 864
- [28] Kohn W and Sham L J 1965 *Phys. Rev. A* **140** 1133
- [29] Becke A D 1988 *Phys. Rev. A* **38** 3098
- [30] Lee C, Yang W and Parr R G 1988 *Phys. Rev.* **B37** 785
- [31] Guest M F, Bush I J, van Dam H J J, Sherwood P, Thomas J M H, van Lenthe J H, Havenith R W A and Kendrick J, Gamess_UK, <http://www.cfs.dl.ac.uk/>
- [32] Frisch M J, Trucks G W, Schlegel H B, Scuseria G E, Robb M A, Cheeseman J R, Montgomery J A, Jr, Vreven T, Kudin K N, Burant J C, Millam J M, Iyengar S S, Tomasi J, Barone V, Mennucci B, Cossi M, Scalmani G, Rega N, Petersson G A, Nakatsuji H, Hada M, Ehara M, Toyota K, Fukuda R, Hasegawa J, Ishida M, Nakajima T, Honda Y, Kitao O, Nakai H, Klene M, Li X, Knox J E, Hratchian H P, Cross J B, Bakken V, Adamo C, Jaramillo J, Gomperts R, Stratmann R E, Yazyev O, Austin A J, Cammi R, Pomelli C, Ochterski J W, Ayala P Y, Morokuma K, Voth G A, Salvador P, Dannenberg J J, Zakrzewski V G, Dapprich S, Daniels A D, Strain M C, Farkas O, Malick D K, Rabuck A D, Raghavachari K, Foresman J B, Ortiz J V, Cui Q, Baboul A G, Clifford S, Cioslowski J, Stefanov B B, Liu G, Liashenko A, Piskorz P, Komaromi I, Martin R L, Fox D J, Keith T, Al-Laham M A, Peng C Y, Nanayakkara A, Challacombe M, Gill P M W, Johnson B, Chen W, Wong M W, Gonzalez C and Pople J A 2004 *Computer code GAUSSIAN 03, revision B.03* (Gaussian, Inc., Wallingford, CT)
- [33] Gopakumar G, Nguyen M T and Ceulemans A 2008 *Chem. Phys. Lett.* **450** 175
- [34] Chacko S, Kanhere D G and Boustani I 2003 *Phys. Rev. B* **68** 035414
- [35] Boustani I, Rubio A and Alonso J A 1999 *Chem. Phys. Lett.* **311** 21
- [36] Boustani I and Quandt A 1997 *Europhys. Lett.* **39** 527
- [37] Boustani I, Quando A and Rubio A 2000 *J. Solid State Chem.* **154** 269
- [38] Kiran B, Bulusu S, Zhai H-J, Yoo S, Zeng X C and Wang L-S 2005 *Proc. Natl. Acad. Sci. U.S.A.* **102** 961
- [39] Marques M A L and Botti S 2005 *J. Chem. Phys.* **123** 014310
- [40] An W, Bulusu S, Gao Y and Zeng X C 2006 *J. Chem. Phys.* **124** 154310
- [41] Oger E, Crawford N R M, Kelting R, Weis P, Kappes M M and Ahlrichs R 2007 *Angew. Chem. Int. Ed.* **46** 8503
- [42] Sergeeva A P, Zubarev D Y, Zhai H-J, Bodyrev A I and Wang L-S 2008 *J. Am. Chem. Soc.* **130** 7244
- [43] Lau K C and Pandey R 2008 *J. Phys. Chem. B* **112** 10217